The brain-specific upregulation of CARD11 in response to avian brain-neurotropic virus infection serves as a potential biomarker

Wenbin Wang ,*,[1] Yajie Zhang,[†] Sa Xiao ,[†] Xuelan Liu,* Peipei Yan,* Chunyan Fu ,* and Zengqi Yang[†]

*Poultry Institute, Shandong Academy of Agricultural Science, Jinan 250100, Shandong, China; and †College of Veterinary Medicine, Northwest A&F University, Yangling 712100, Shaanxi, China

ABSTRACT Avian neurotropic viruses are critical problems in poultry industry causing severe central nervous system (**CNS**) damage with neuroinvasive and neurovirulence properties. Biomarker of neurotropic viral intracranial invasion is of great application value for the diagnosis, but that of avian neurotropic viruses remains elusive. Previously, we found that chicken caspase recruitment domain family, member 11 (**CARD11**) was only upregulated in virulent Newcastle disease virus-infected chickens and in chicken primary neuronal cells. In this study, CARD11 was systemically expressed in chickens and pigeons detected by absolute qPCR and immunohistochemical (**IHC**) assay. After virus challenging, only avian neurotropic viruses (avian encephalomyelitis virus [**AEV**] and pigeon paramyxovirus type 1 [**PPMV-1**]) except Marek's disease virus (**MDV**) can invade brain and cause pathological changes. The relative mRNA expression of CARD11 was brain-upregulated in AEV- or PPMV-1-infected animals, rather than MDV and non-neurotropic viruses (fowl adenovirus serotype 4 [**FAdV-4**] and infectious bronchitis virus [**IBV**]). Similarly, the protein expression of CARD11 was only upregulated in the cerebra and cerebella infected by avian brain-neurotropic virus using IHC assay. And there were no correlations between the change level of CARD11 and viral load. Our preliminary data suggested that avian CARD11 may be a potential brain biomarker for avian brain-neurotropic virus invasion.

Key words: CARD11, brain-specific upregulation, avian brain-neurotropic virus, potential biomarker

2023 Poultry Science 102:102539
https://doi.org/10.1016/j.psj.2023.102539

INTRODUCTION

Neurotropic virus can specifically invade the central nervous system (**CNS**), causing severe disease with both neuroinvasive and neurovirulence properties and has serious effects on human and animal health (Abdullahi et al., 2020). At present, biomarkers detected directly from the cerebrospinal fluid (**CSF**), plasma, brain, or spinal cord are useful to characterize the CNS responses associated with pathogenic infections. For instance, glial fibrillary acidic protein and light subunit of neurofilament protein are CSF biomarkers that have been used to estimate the severity of the brain damage and the outcomes in varicella zoster virus (Grahn et al., 2013) and SARS-CoV-2 infections (Virhammar et al., 2021). Concentrations of kynurenine and biogenic amines as potential CSF biomarkers are significantly increased in herpes simplex virus CNS infection (Taj and Jamil, 2018; Suhs et al., 2019). Karyopherin alpha 4 in the human brain (Mehta et al., 2015) and Fas ligand in the spinal cord (Baloul et al., 2004) are biomarkers of rabies virus infection. Avian paramyxovirus serotype 1 (**APMV-1**) (Dortmans et al., 2011), avian encephalomyelitis virus (**AEV**) (Liu et al., 2014), highly pathogenic avian influenza virus (**HPAIV**) (Chaves et al., 2011), and Marek's disease virus (**MDV**) (Cho et al., 1998) can invade the nervous system and induce neurological symptoms in poultry. The first 3 mainly infect the CNS, and MDV mainly infects the peripheral nervous system. However, biomarkers of avian neurotropic viruses remain elusive.

Previously, we discovered that chicken caspase recruitment domain family, member 11 (**CARD11**) was only significantly upregulated in virulent Newcastle disease virus (**VNDV**), an F48E9 strain (Genbank Accession Number: MG456905), infected chicken brains and primary neuronal cells (Wang et al., 2019). CARD11, also called caspase recruitment domain-

Received September 16, 2022.
Accepted January 20, 2023.

[1]Corresponding author: wangwenbin1230@163.com

containing C-terminal membrane-associated guanylate kinase (**MAGUK**) protein-1 (**CARMA1**), is mainly expressed in mammal lymphatic organs, which interacts with B-cell lymphoma/leukemia 10 (**Bcl10**) and mucosa-associated lymphoid organ lymphoma translocation protein 1 (**MALT1**) to form the CARD11-Bcl10-MALT1 (**CBM**) complex and regulates the proliferation of lymphocytes via activating the nuclear factor κ (**NF-κB**), c-Jun N-terminal kinase (**JNK**), and mammalian target of rapamycin (**mTOR**) (Bedsaul et al., 2018; Lork et al., 2019). The mutation and dysregulation of CARD11 in lymphocytes causes diseases, such as various lymphomas and primary immunodeficiency (Turvey et al., 2014; Brohl et al., 2015). Considering this, we here investigated the relationship between the expression changes of CARD11 in the brain and avian neurotropic virus invasion.

In this study, we first show that CARD11 is expressed systemically in both chickens and pigeons using absolute qPCR and immunohistochemical (**IHC**) assay. To determine the relative expression of CARD11 in other avian neurotropic viruses infected organs, we chose AEV, Marek's disease virus (**MDV**), pigeon paramyxovirus type 1 (**PPMV-1**), belonging to APMV-1, to infect specific pathogen-free (**SPF**) chickens and pigeons. Meanwhile, fowl adenovirus serotype 4 (**FAdV-4**) and infectious bronchitis virus (**IBV**) as the non-neurotropic virus models were used to infect SPF chickens. The relative expression of CARD11 mRNA and protein were significantly upregulated only in cerebrum and cerebellum induced by AEV or PPMV-1 infection but not MDV, FAdV-4 or IBV infection. In all the animal challenge experiments, there was no inevitable association between pathological changes and viral load of avian neurotropic virus-infected brains. These outcomes suggest that avian CARD11 is brain-specific upregulated induced by avian neurotropic viruses with the ability to invade the brain, and it may be a potential biomarker for avian brain-neurotropic virus infection of CNS.

MATERIALS AND METHODS

Ethics Statement

This study was carried out in strict accordance with the recommendations in the Guide for the Care and Use of Laboratory Animals of the Ministry of Science and Technology of the People's Republic of China. All animal experiments were reviewed and approved by the Animal Ethics and Welfare Committee of Northwest A&F University, and accords with the principles of animal protection, animal welfare and ethics, as well as the relevant provisions of national laboratory animal welfare ethics (Approval numbers: 2019ZX01001007-001 and 2022ZX11025002-004 for SPF chickens, 2021ZX04005008-002 for pigeons).

Viruses and Animals

The AEV strain XY/Q-1410 (GenBank accession no. NC_003990) (Fan et al., 2017), the PPMV-1 strain GS02 isolate (GenBank accession no. OM640464) (Zhang et al., 2022), the FAdV-4 strain SXD15 (Wang et al., 2018), and the IBV strain CK/CH/Shaanxi/2009/H09 (GenBank accession no. KC478643) were propagated and stored at −80°C by our laboratory after being isolated. The very virulent MDV (**vvMDV**) strain Md5 (GenBank accession no. AF243438) (Reddy et al., 2002) was gifted from Prof. Peng Zhao (Shandong Agricultural University). All 9- to 11-day-old SPF embryonated chicken eggs and SPF white Leghorn chickens were supplied from Shandong Healthteach Laboratory Animal Breeding Co., Ltd. (Jinan, China). All pigeons were purchased from a pigeon farm in Yangling, China and were housed in isolators throughout the experiments. Adequate food and drinking water were provided. All pigeons were confirmed without antibodies against NDV by performing hemagglutination inhibition (**HI**) tests on the days before the experiments.

Animal Challenge Experiments

The detailed challenge experiment protocols were shown in Table 1. The negative control group received the same volume of phosphate-buffered saline (**PBS**) solution at pH 7.2. All animals were observed daily. Bleeding of the animals was performed under anesthesia using ketamine and xylazine. And all the challenged animals were euthanized with carbon dioxide when they became moribund. The pathological changes in all the organs were evaluated during necropsy. The organs were collected for further pathological analysis and DNA/RNA extraction.

Table 1. The different virus challenge experiments.

Virus	Isolation	Animal age	Animal number/group	Inoculation route	Inoculation dose/animal
Mock	sterile PBS	3-wk-old SPF chickens	10	o.n. or i.m. or i.p.	100 μL
IBV	H09			o.n.	10^6 EID_{50}/100 μL
FAdV-4	SXD15			i.m.	10^5 $TCID_{50}$/100 μL
AEV	XY/Q-1410	1-day-old SPF chicks		o.n.	10^5 EID_{50}/100 μL
MDV	Md5			i.p.	1000 pfu/100 μL
Mock	sterile PBS	3-mo-old pigeons		o.n.	100 μL
PPMV-1	GS02				10^6 pfu/100 μL

Abbreviations: o.n., intraocular-nasal route; i.m., intramuscular injection; i.p., intraperitoneal injection.

Table 2. The details of the real-time qPCR.

Gene	Primer	5'→3' sequence	Length (bp)	Standard curve
chCARD11	forward reverse	GCTTCTGACACGGCAGCATCT CATTTCCTTTAGCCCAATCCTC	195	y=39.846-3.153x (R^2 = 0.9963)
pCARD11	forward reverse	AAATTAACCGAGCAGGCCGA CGCTGCACATCTTTTGCCTT	241	y=35.655-3.023x (R^2 = 0.9952)
PPMV-1 NP	forward reverse	CAACAACAGGAGTGGAGTGTCTGA TAGAGTATCAGTGATATCTTCT	145	y=39.961-3.398x (R^2 = 0.999)
AEV VP1	forward reverse	GAATTAGCTCCTGGTAAACCTCG TATTATCGCAACACCCTCAGG	288	y=36.754-3.5714x (R^2 = 0.9977)
MDV Meq	forward reverse	GACGCCGCTCGGAGAAGAC CCATAGGGCAAACTGGCTCAT	175	Y=36.90-3.3721x (R^2 = 0.999)
FAdV-4 hexon	forward reverse	CGTCAACTTCAAGTACTC AGAGGATGCTCATGTTAC	86	y=38.305-3.1077x (R^2 = 0.9951)
IBV N	forward reverse	CAGGACCAGCCGCTAACCTGAAT AATCTTAGCCGCACGAGCTATA	317	y=38.673-3.455x (R^2 = 0.994)
chicken 28S rRNA	forward reverse	CCGATGCCGACGCTCAT GGTATGGGCCCGACGCT	159	-
pigeon GAPDH	forward reverse	TGCCTCTTGCACTACTAACTGCC TCATAAGACCCTCCACGATGCC	121	-

-: no standard curve.

Establishment of Standard Curve For qPCR

A standard curve was established with serially diluted plasmids (10^2–10^8 copies/μL) that harbored the CARD11 gene. The PCR product size was 195 bp for chicken CARD11 (**chCARD11**) and 241 bp for pigeon CARD11 (**pCARD11**), and the primers were shown in Table 2. The Applied Biosystem QuantStudi 6 Flex Real-Time PCR System (Applied Biosystems, Waltham, MA) was used to generate the standard curve. qPCR detection was performed in triplicate for each sample independently using EvaGreen 2 × qPCR MasterMix-ROX (Applied Biological Materials, Vancouver, Canada). Absolute quantification of CARD11 mRNA copies was determined by comparison with the standard curve. A melting curve analysis was used to evaluate the amplification result. The standard curve of AEV VP1 gene, PPMV-1 NP gene, MDV Meq, FADV-4 hexon gene, IBV N gene were established previously (Fan et al., 2017; Yu et al., 2018; Wang et al., 2021).

Real-Time qPCR

Total RNA or viral DNA of the virus-infected organs was isolated using E.Z.N.A. Viral DNA Kit (OMEGA, Norcross, GA) and TRI Gene Reagent (GenStar, China), respectively. To measure the DNA synthesis of MDV and FAdV-4, 500 ng of extracted DNA was used for Real-time qPCR with specific primers (Table 2). To measure CARD11 mRNA and mRNA synthesis of AEV, PPMV-1, and IBV, 3 μg of extracted RNA was reverse-transcribed using the StarScript II First-strand cDNA Synthesis Kit (GenStar) with oligo(dT) primers. The real-time qPCR was performed on an Applied Biosystem QuantStudi 6 Flex Real-Time PCR System (Applied Biosystems) using EvaGreen 2 × qPCR MasterMix-ROX (Applied Biological Materials) with specific primers (Table 2). The copies of DNA or mRNA per gram of organ were calculated using the established standard curves shown in Table 2. The relative mRNA level of CARD11 was normalized to those of the corresponding chicken 28S rRNA or pigeon GAPDH and calculated by the comparative threshold cycle ($\Delta\Delta$Ct) method. The ratios of gene expression between the treatment and control samples were calculated as $2^{-\Delta\Delta Ct}$.

Histopathology and IHC Assays

The HE and IHC assays were performed by Shaanxi Yike Biotechnology Service Co., Ltd. All the harvested organs were fixed in phosphate-buffered formalin (10%), embedded in paraffin, and sectioned. The organs were deparaffinized, rehydrated, and subsequently stained with HE. The IHC assay was performed to detect the presence of CARD11 protein using anti-chCARD11 mouse pAb (1:500) which had been previously prepared by our lab (Wang et al., 2019). The anti-chCARD11 mouse pAb could be used for detecting pCARD11 since the amino acid of pCARD11 and chCARD11 was highly homologous (almost 94%). All the samples were observed and photographed using a Nikon Ni-U microscope. The expression level of CARD11 protein in IHC assay was analyzed by average optical density using ImageJ software.

Statistical Analysis

Two-tailed Student's t test was used to estimate the statistical significance between 2 columns in Prism 8.0 software (GraphPad Inc., San Diego, CA). Data from 3 independent experiments are presented as the means ± standard deviations (**SD**); $P < 0.05$ was considered statistically significant.

RESULTS

CARD11 is Expressed Systemically in Both Chickens and Pigeons

To identify the content of chCARD11 and pCARD11 mRNA in the normal organs, standard curves were y = 39.846-3.153x and y = 35.655-3.023x, respectively (Table 2). The expression of chCARD11 mRNA was higher in the kidney, bursa, and spleen, and lower in the pancreas (Figure 1A), and pCARD11 mRNA expression was highest in the pancreas and lowest in muscle (Figure 1B). Because CARD11 in organs cannot be detected via western blotting using the anti-chCARD11 antibody, to further confirm the expression of CARD11, the protein level of CARD11 was confirmed via IHC assay. ChCARD11 and pCARD11 protein was expressed systemically (Figures 2A and 2C). The average optical density (**AOD**) of IHC photographs showed that the expression of chCARD11 was higher in the muscular stomach, liver, and glandular stomach, and lower in the pancreas and muscle (Figure 2B), and that of pCARD11 was higher in the pancreas and liver, and lower in the cerebellum and muscle (Figure 2D). These results suggested that the distribution of CARD11 in different avian organs was not consistent. Unlike mammalian CARD11 expression, avian CARD11 is not predominantly expressed in lymphoid organs (Bedsaul et al., 2018; Wei et al., 2019), indicating that avian CARD11 might play a special biological function.

Avian Brain-Neurotropic Virus Has the Property of Intracranial Invasion

For AEV infection, the chicks showed depression, inappetence, and ataxia. Necropsies of the sick chicks showed severe encephalomalacia and hemorrhage (Figure 3). No significant changes were observed in the other organs. The PPMV-1-infected pigeons exhibited head tremor, twisted neck, and unilateral or bilateral wing paralysis. Encephalomalacia and severe hemorrhage in the cerebellum were seen in challenged pigeons (Figure 3). In addition, the glandular stomach nipples were collapsed and slight hemorrhage. The liver was swollen and friable with patchy hemorrhage, and the trachea was swollen. The MDV-infected chicks appeared depression and ataxia with leg "split" position. Necropsies showed slight vascular congestion in the cerebrum (Figure 3), severe atrophied thymus and bursae, and tumor lesion in liver. As control, no damage was shown in the FAdV-4- or IBV-infected chicken brains (Figure 3). Using HE assays, perivascular lymphocytic cuffing and edema in the cerebrum and cerebellar cortex, and irrobegular cerebellar stratum granulosum were observed in the AEV or PPMV-1 infection group, and there was no pathological change in the MDV-infected brain (Figure 4). Glandular papillary hemorrhage in the glandular stomach of PPMV-1 infection (Figure 4) was similar to VNDV. Although the pathological changes of cerebrum and cerebellum in the AEV- or PPMV-1-infected group were obvious, the viral loads were not the highest (Figure 5), suggesting that there was little association between viral load and pathological changes of avian neurotropic virus-infected brains. The viral loads of FAdV-4- or IBV-infected chicken brains were very low and consistent with pathological changes (Figure 5). These results confirmed that avian brain-neurotropic virus, AEV, NDV, or PPMV-1, can invade CNS.

CARD11 is Brain-Specific Upregulated Induced by Avian Brain-Neurotropic Virus

First, we found that the relative mRNA expression of CARD11 was significantly upregulated only in cerebrum and cerebellum induced by AEV or PPMV-1 infection

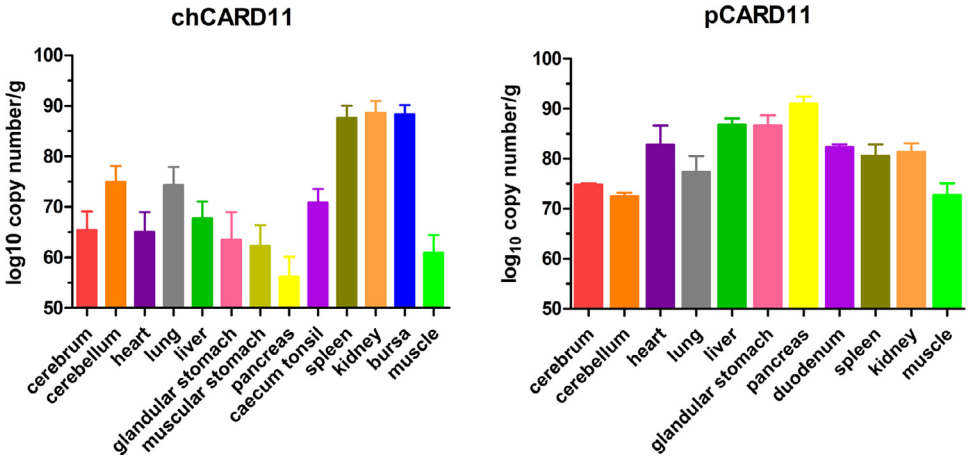

Figure 1. The mRNA expression of CARD11 in chickens and pigeons. Three-week-old SPF white Leghorn chickens and 3-month-old pigeons were euthanized with carbon dioxide. The total RNA was extracted from the organs. The mRNA copy numbers per g of organ of chCARD11 (A) and pCARD11 (B) were calculated using the established standard curves. The results are presented as the mean ± SD.

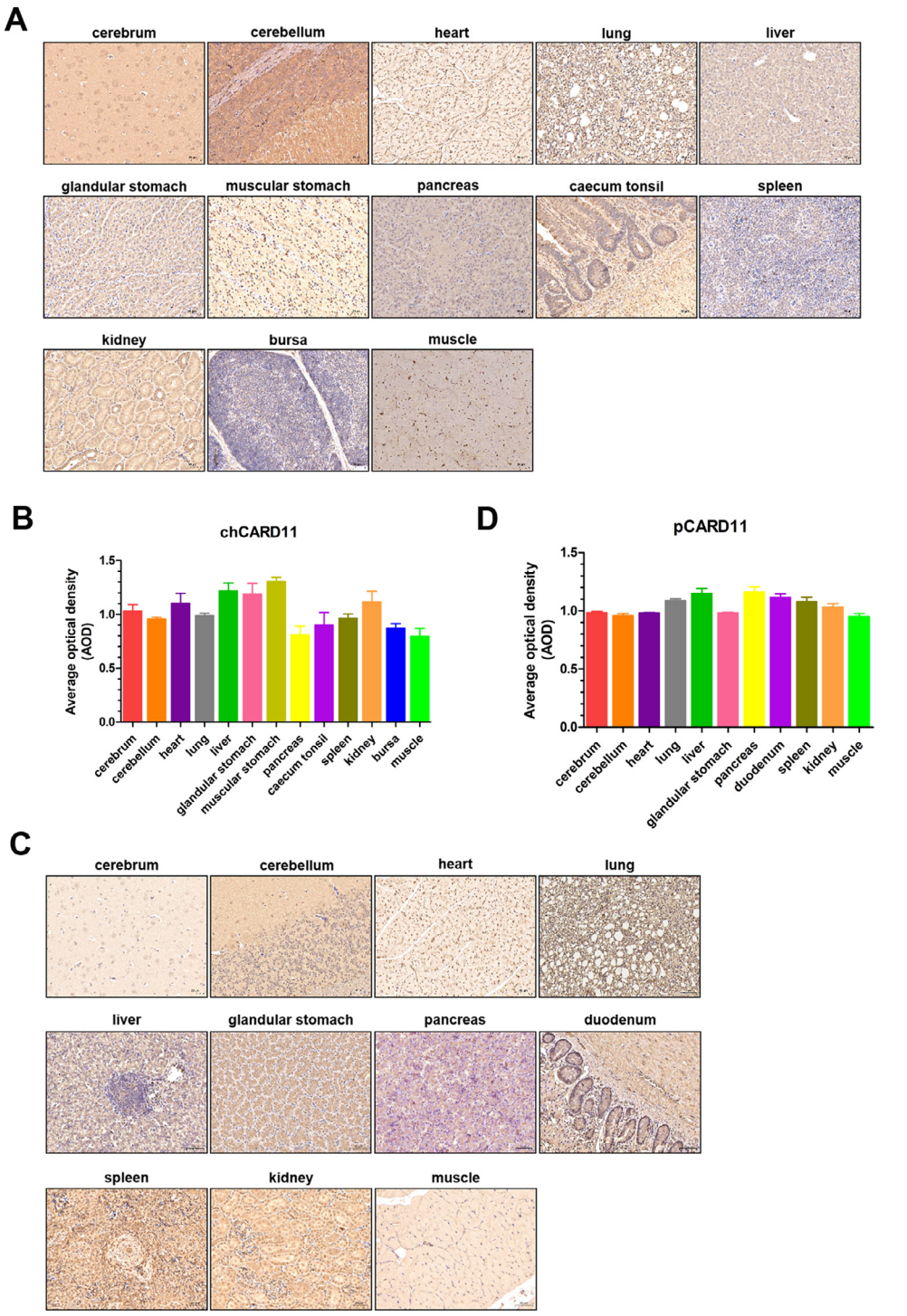

Figure 2. The protein expression of CARD11 in normal chickens and pigeons. IHC assay of different chicken (A) and pigeon (C) organs was performed using anti-chCARD11 mouse pAb (1:500) prepared previously for detecting chCARD11 and pCARD11. Scale bar = 50 μm. (B, D) The AOD of IHC photographs was analyzed using ImageJ software.

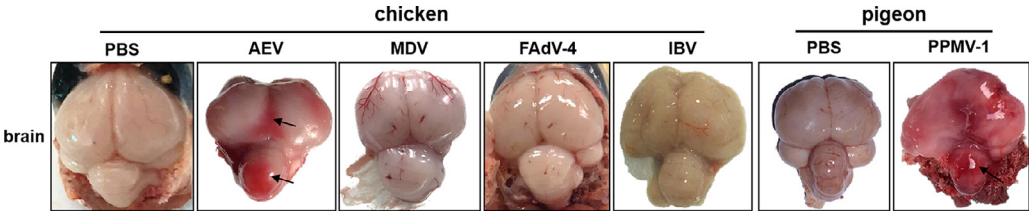

Figure 3. Gross lesions of cerebrum and cerebellum in the virus challenged animals. The black arrows indicate the indistinct boundary between the cerebrum and cerebellum, and hemorrhage, respectively.

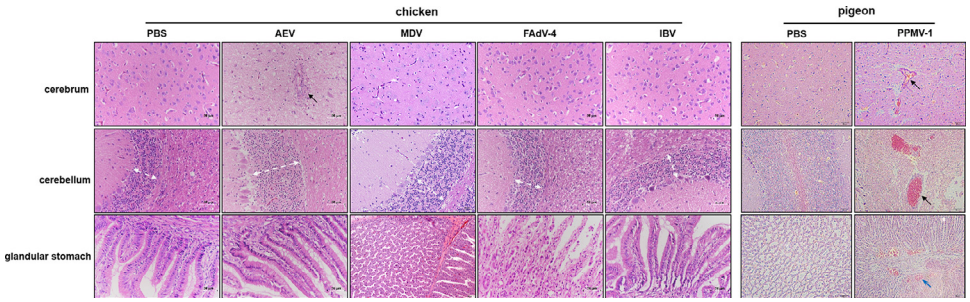

Figure 4. Histopathology of cerebrum, cerebellum, and glandular stomach in the virus challenged animals. Tissues were fixed with 4% paraformaldehyde fixative, sectioned, and stained with hematoxylin and eosin. The histological lesions were as follows: perivascular lymphocytic cuffing in the cerebral and cerebellar cortex (black arrows). Thickness of the stratum granulosum in the cerebellum (white double dotted arrows). glandular papillary hemorrhage in the glandular stomach (blue arrowhead). Scale bar = 50 μm.

but not MDV, FAdV-4, or IBV infection (Figure 6). After virus challenges, the expression of chCARD11 and pCARD11 were upregulated in the cerebrum and cerebellum of AEV- and PPMV-1-infected animals rather than the MDV, FAdV-4, and IBV groups (Figure 7A). The upregulation of CARD11 was only in the brains rather than in the glandular stomachs (Figure 7B). These results indicated that avian CARD11 is brain-specific upregulated induced by avian brain-neurotropic virus, and may be a potential brain biomarker for intracranial invasion of avian neurotropic virus.

DISCUSSION

From animal welfare, avian neurotropic virus infection of the CNS is a severe problem that affects the animal quality of life and has direct repercussions on poultry production. In avian neurophilic virus, AEV, APMV-1, and HPAIV are able to invade brain (Chaves et al., 2011; Dortmans et al., 2011; Liu et al., 2014). In this research, we determined that MDV does not cause brain damage (Figures 3 and 4). The pathological change of sciatic nerve in MDV-infected chicks, such as edema, separation between nerve fibers and extravascular lymphocyte infiltration, resulted in ataxia with leg "split" position. And we observed that the animals challenged with APMV-1 and AEV showed ataxia, such as head tremor, twisted neck, unilateral or bilateral wing paralysis, and limping, suggesting that avian brain-neurotropic viruses may be more likely to invade the cerebellum than the cerebrum. Besides, CARD11 was upregulated in the Purkinje cells of the cerebellum under AEV and PPMV-1 challenge (Figure 7A). As we know, Purkinje cells are the sole output neurons of the cerebellar cortex and thus changes in their function have a significant impact on the function of the cerebellum as a whole. Once damaged, neurological symptoms such as ataxia occurs (Redondo et al., 2015). And previous research reported that degeneration of Purkinje cells was observed in NDV-infected brain (Subbaiah et al., 2011). These findings guide our future research on the role of CARD11 in a different type of neuronal cells, especially suggesting that CARD11 has a special role in Purkinje cells.

To apply CARD11 as a biomarker for brain-neurotropic virus infection and facilitate clinical detection, the expression changes of CARD11 in peripheral blood lymphocytes (**PBLC**) after APMV-1 and AEV infection were determined. Unexpectedly, it was not upregulated in PBLC (data not shown). Furthermore, we also detected that CARD11 was not upregulated in the spinal cord (data not shown). So at present, CARD11 can only be used as a brain biomarker for avian brain-neurotropic virus infection. In addition, the expression changes of CARD11 in mammalian neurotropic virus infection were examined. Surprisingly, we found that CARD11 was only upregulated in the mouse brain respectively infected with pseudorabies virus, Zika virus, and Japanese encephalitis virus (data not shown). These preliminary results suggested that the brain-specific upregulation of CARD11 after neurotropic virus infection is universal and further study is required to validate and broaden our founding regarding mammalian neurotropic virus.

In summary, based on our previous research on virulent NDV infection, we found that CARD11 was expressed systemically in chickens and pigeons. After animal challenge experiments, both mRNA and protein levels of CARD11 were only upregulated in the cerebrum and cerebellum of animals infected with avian brain-neurotropic viruses, AEV and PPMV-1, rather than in MDV and avian non-neurotropic viruses, FAdV-4 and IBV. There were no correlations between the change level of CARD11 and viral load. Overall, our preliminary data can indicate that CARD11 has the potential to be used as a CNS biomarker for brain-neurotropic virus invasion.

ACKNOWLEDGMENTS

This work was supported by the Natural Science Foundation of Shandong Province [grant number ZR2021QC185 to WW]; the Agricultural Science and Technology Innovation Project of Shandong Academy

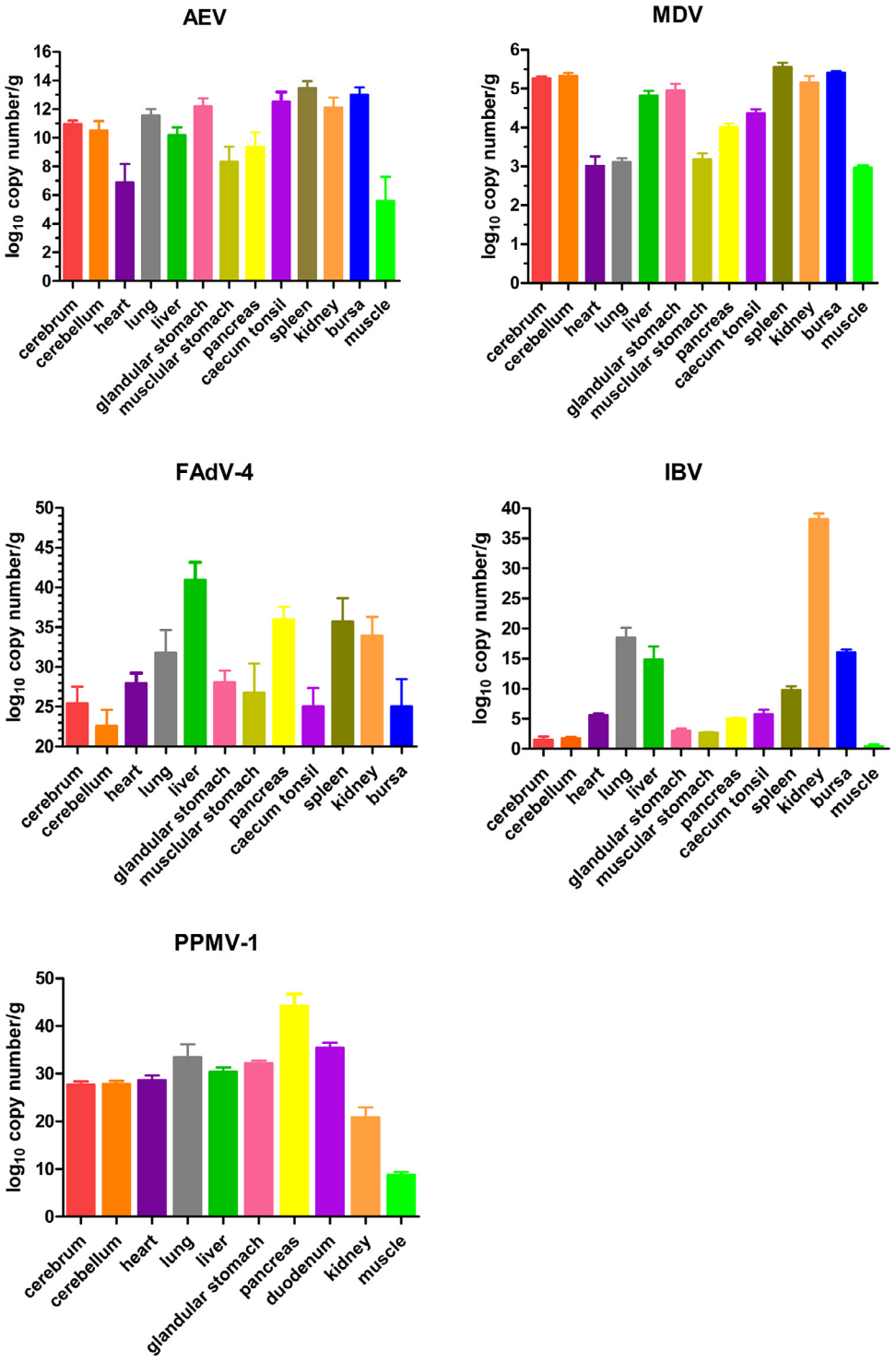

Figure 5. Viral loads in different organs of the virus challenged animals. The mRNA or DNA copies of different viral genes in the virus-infected animals were determined by RT-qPCR and were calculated using the established standard curves in Table 1. The results are presented as the mean ± SD.

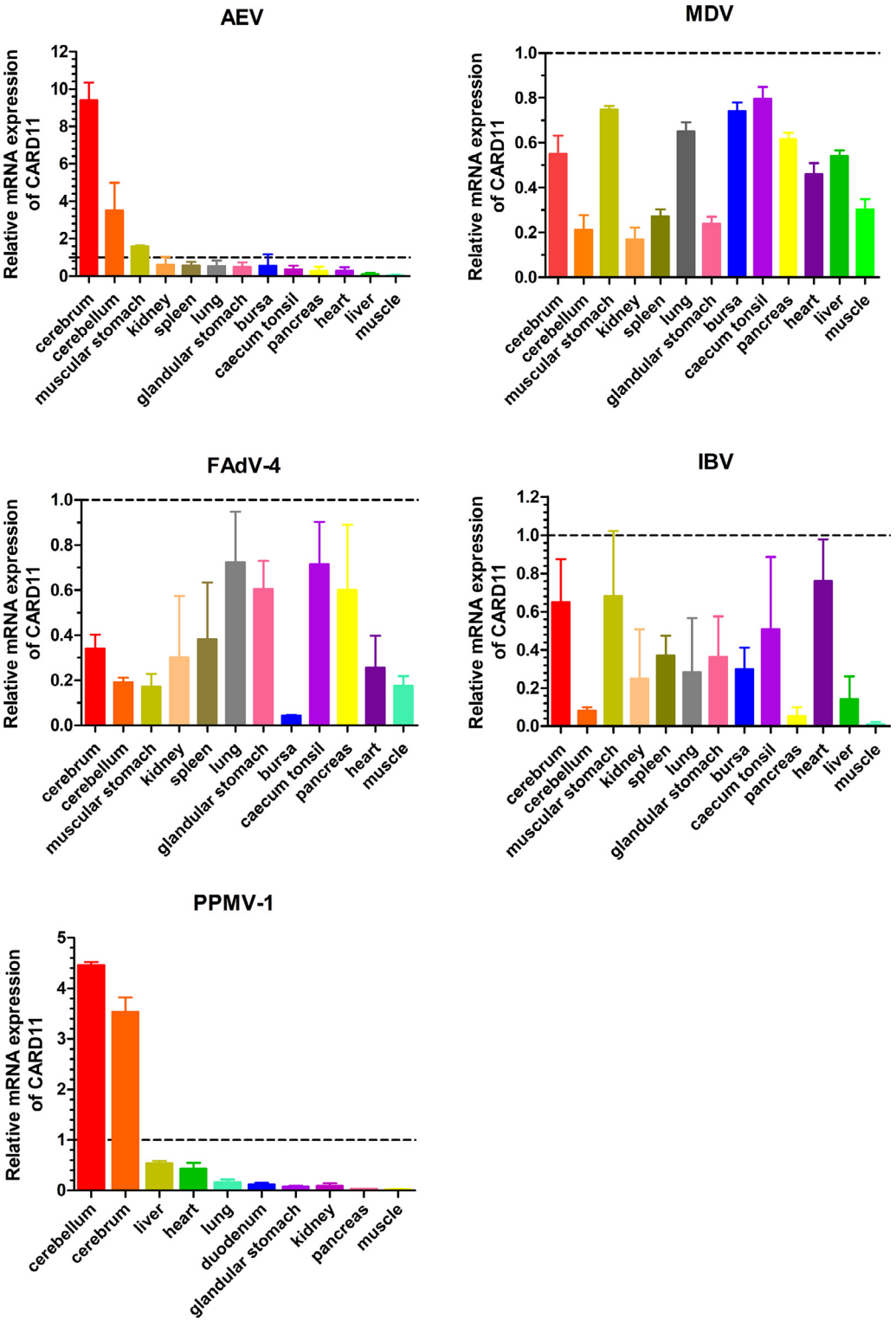

Figure 6. The relative mRNA expression of CARD11 in different organs of the virus challenged animals. The relative mRNA expression of chCARD11 and pCARD11 was determined by RT-qPCR and was normalized to that of 28S rRNA and GAPDH, respectively. The results are presented as the mean ± SD.

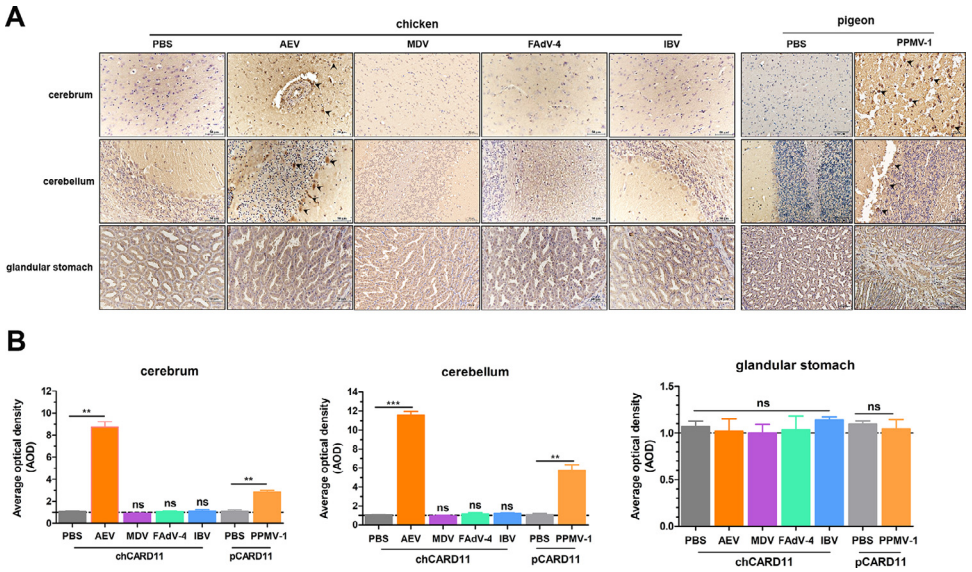

Figure 7. IHC assay of cerebrum, cerebellum, and glandular stomach in the virus challenged animals. (A) The anti-chCARD11 mouse pAb (1:500) prepared previously was used for detecting chCARD11 and pCARD11. The black arrowheads represent the position of CARD11. Scale bar = 50 μm. (B) The AOD of IHC photographs was analyzed using ImageJ software. The results are presented as the mean ± SD of three independent experiments and were analyzed by two-tailed Student's *t* test. $^{*}P < 0.05$, $^{**}P < 0.01$, $^{***}P < 0.001$. Abbreviations: IHC, immunohistochemical; ns, not significant.

of Agricultural Sciences [grant number CXGC2021B22 to WW]; and the National Natural Science Foundation of China [grant number 31572533 to SX].

DISCLOSURES

The authors declare that they have no known competing financial interests or personal relationships that could have appeared to influence the work reported in this paper.

REFERENCES

Abdullahi, A. M., S. T. Sarmast, and R. Singh. 2020. Molecular biology and epidemiology of neurotropic viruses. Cureus 12:e9674.

Baloul, L., S. Camelo, and M. Lafon. 2004. Up-regulation of Fas ligand (FasL) in the central nervous system: a mechanism of immune evasion by rabies virus. J. Neurovirol. 10:372–382.

Bedsaul, J. R., N. M. Carter, K. E. Deibel, S. M. Hutcherson, T. A. Jones, Z. Wang, C. Yang, Y. K. Yang, and J. L. Pomerantz. 2018. Mechanisms of regulated and dysregulated CARD11 signaling in adaptive immunity and disease. Front. Immunol. 9:2105.

Brohl, A. S., J. R. Stinson, H. C. Su, T. Badgett, C. D. Jennings, G. Sukumar, S. Sindiri, W. Wang, L. Kardava, S. Moir, C. L. Dalgard, J. A. Moscow, J. Khan, and A. L. Snow. 2015. Germline CARD11 mutation in a patient with severe congenital B cell lymphocytosis. J. Clin. Immunol. 35:32–46.

Chaves, A. J., N. Busquets, R. Valle, R. Rivas, J. Vergara-Alert, R. Dolz, A. Ramis, A. Darji, and N. Majo. 2011. Neuropathogenesis of a highly pathogenic avian influenza virus (H7N1) in experimentally infected chickens. Vet. Res. 42:106.

Cho, K. O., D. Endoh, J. F. Qian, K. Ochiai, M. Onuma, and C. Itakura. 1998. Central nervous system lesions induced experimentally by a very virulent strain of Marek's disease virus in Marek's disease-resistant chickens. Avian. Pathol. 27:512–517.

Dortmans, J. C., G. Koch, P. J. Rottier, and B. P. Peeters. 2011. Virulence of Newcastle disease virus: what is known so far? Vet. Res. 42:122.

Fan, L., Z. Li, J. Huang, Z. Yang, S. Xiao, X. Wang, R. Dang, and S. Zhang. 2017. Dynamic distribution and organ tropism of avian encephalomyelitis virus isolate XY/Q-1410 in experimentally infected Korean quail. Arch. Virol. 162:3447–3458.

Grahn, A., L. Hagberg, S. Nilsson, K. Blennow, H. Zetterberg, and M. Studahl. 2013. Cerebrospinal fluid biomarkers in patients with varicella-zoster virus CNS infections. J. Neurol. 260:1813–1821.

Liu, Q., Z. Yang, H. Hao, S. Cheng, W. Fan, E. Du, S. Xiao, X. Wang, and S. Zhang. 2014. Development of a SYBR Green real-time RT-PCR assay for the detection of avian encephalomyelitis virus. J. Virol. Methods 206:46–50.

Lork, M., J. Staal, and R. Beyaert. 2019. Ubiquitination and phosphorylation of the CARD11-BCL10-MALT1 signalosome in T cells. Cell. Immunol. 340:103877.

Mehta, S. M., S. M. Banerjee, and A. S. Chowdhary. 2015. Postgenomics biomarkers for rabies-the next decade of proteomics. OMICS 19:67–79.

Reddy, S. M., B. Lupiani, I. M. Gimeno, R. F. Silva, L. F. Lee, and R. L. Witter. 2002. Rescue of a pathogenic Marek's disease virus with overlapping cosmid DNAs: use of a pp38 mutant to validate the technology for the study of gene function. Proc. Natl. Acad. Sci. U. S. A 99:7054–7059.

Redondo, J., K. Kemp, K. Hares, C. Rice, N. Scolding, and A. Wilkins. 2015. Purkinje cell pathology and loss in multiple sclerosis cerebellum. Brain. Pathol. 25:692–700.

Subbaiah, K. C., D. Rajanipramila, G. Visweswari, W. Rajendra, and V. Lokanatha. 2011. Perturbations in the antioxidant metabolism during Newcastle disease virus (NDV) infection in chicken: protective role of vitamin E. Naturwissenschaften 98:1019–1026.

Suhs, K. W., N. Novoselova, M. Kuhn, L. Seegers, V. Kaever, K. Muller-Vahl, C. Trebst, T. Skripuletz, M. Stangel, and F. Pessler. 2019. Kynurenine is a cerebrospinal fluid biomarker for bacterial and viral central nervous system infections. J. Infect. Dis. 220:127–138.

Taj, A., and N. Jamil. 2018. Cerebrospinal fluid concentrations of biogenic amines: potential biomarkers for diagnosis of bacterial and viral meningitis. Pathogens 7:39.

Turvey, S. E., A. Durandy, A. Fischer, S. Y. Fung, R. S. Geha, A. Gewies, T. Giese, J. Greil, B. Keller, M. L. McKinnon, B. Neven, J. Rozmus, J. Ruland, A. L. Snow, P. Stepensky, and K. Warnatz. 2014. The CARD11-BCL10-MALT1 (CBM) signalosome complex: stepping into the limelight of human primary immunodeficiency. J. Allergy. Clin. Immunol. 134:276–284.

Virhammar, J., A. Naas, D. Fallmar, J. L. Cunningham, A. Klang, N. J. Ashton, S. Jackmann, G. Westman, R. Frithiof, K. Blennow, H. Zetterberg, E. Kumlien, and E. Rostami. 2021. Biomarkers for

central nervous system injury in cerebrospinal fluid are elevated in COVID-19 and associated with neurological symptoms and disease severity. Eur. J. Neurol. 28:3324–3331.

Wang, W., Q. Wei, Q. Hao, Y. Zhang, Y. Li, Y. Bi, Z. Jin, H. Liu, X. Liu, Z. Yang, and S. Xiao. 2021. Cellular CARD11 inhibits the fusogenic activity of newcastle disease virus via CBM signalosome-mediated furin reduction in chicken fibroblasts. Front. Microbiol. 12:607451.

Wang, W., X. Chang, W. Yao, N. Wei, N. Huo, Y. Wang, Q. Wei, H. Liu, X. Wang, S. Zhang, Z. Yang, and S. Xiao. 2019. Host CARD11 inhibits Newcastle disease virus replication by suppressing viral polymerase activity in neurons. J. Virol. 93:01499-19.

Wang, X., Q. Tang, Z. Chu, P. Wang, C. Luo, Y. Zhang, X. Fang, L. Qiu, R. Dang, and Z. Yang. 2018. Immune protection efficacy of FAdV-4 surface proteins fiber-1, fiber-2, hexon and penton base. Virus. Res. 245:1–6.

Wei, Z., Y. Zhang, J. Chen, Y. Hu, P. Jia, X. Wang, Q. Zhao, Y. Deng, N. Li, Y. Zang, J. Qin, X. Wang, and W. Lu. 2019. Pathogenic CARD11 mutations affect B cell development and differentiation through a noncanonical pathway. Sci. Immunol. 4:5618.

Yu, G., Y. Wang, M. Zhang, Y. Lin, Y. Tang, and Y. Diao. 2018. Pathogenic, phylogenetic, and serological analysis of group I fowl adenovirus serotype 4 SDSX isolated from shandong. China. Front. Microbiol. 9:2772.

Zhang, Y., W. Wang, Y. Li, J. Liu, W. Wang, J. Bai, Z. Yang, H. Liu, and S. Xiao. 2022. A pigeon paramyxovirus type 1 isolated from racing pigeon as an inactivated vaccine candidate provides effective protection. Poult. Sci. 101:102097.